Novel High-Pressure Yttrium Carbide γ-Y_4C_5 Containing $[C_2]$ and Nonlinear $[C_3]$ Units with Unusually Large Formal Charges

Alena Aslandukova[1,*] Andrey Aslandukov,[2] Liang Yuan,[1] Dominique Laniel,[2] Saiana Khandarkhaeva,[2]
Timofey Fedotenko,[2] Gerd Steinle-Neumann,[1] Konstantin Glazyrin,[3] Natalia Dubrovinskaia,[2,4] and Leonid Dubrovinsky[1]

[1]*Bavarian Research Institute of Experimental Geochemistry and Geophysics, University of Bayreuth, 95440 Bayreuth, Germany*
[2]*Material Physics and Technology at Extreme Conditions, Laboratory of Crystallography,*
University of Bayreuth, 95440 Bayreuth, Germany
[3]*Photon Science, Deutsches Elektronen-Synchrotron, Notkestrasse 85, 22607 Hamburg, Germany*
[4]*Department of Physics, Chemistry and Biology (IFM), Linköping University, SE-581 83 Linköping, Sweden*

Changes in the bonding of carbon under high pressure leads to unusual crystal chemistry and can dramatically alter the properties of transition metal carbides. In this work, the new orthorhombic polymorph of yttrium carbide, γ-Y_4C_5, was synthesized from yttrium and paraffin oil in a laser-heated diamond anvil cell at ~50 GPa. The structure of γ-Y_4C_5 was solved and refined using *in situ* synchrotron single-crystal x-ray diffraction. It includes two carbon groups: $[C_2]$ dimers and nonlinear $[C_3]$ trimers. Crystal chemical analysis and density functional theory calculations revealed unusually high noninteger charges ($[C_2]^{5.2-}$ and $[C_3]^{6.8-}$) and unique bond orders (<1.5). Our results extend the list of possible carbon states at extreme conditions.

Introduction.—Metal carbides exhibit high melting points, high hardness, and metallic conductivity that make them attractive candidates for different technological applications in material science [1]. Carbon has the capability of forming various bond states affecting the structures and properties of transition metal carbides [2]. Most metal carbides are either substitutional or interstitial solid solutions, or they form binary compounds with simple crystal structures (e.g., of a rock salt type) [3]. However, more complex carbides with covalent C-C bonds are also known.

There is a large number of metal carbides containing $[C_2]$ dimers, for example, CaC_2, SrC_2, BaC_2, YC_2, LaC_2, La_2C_3, CeC_2, TbC_2, YbC_2, and LuC_2 [4–7]. The C-C bond length in these carbides depends on the charge of the cation and increases proportionally with the valence of the metal [8–10]. The crystal chemistry of carbides containing triatomic $[C_3]$ units is much more varied. The $[C_3]$ unit was suggested to be in Li_4C_3 [11] and is known to exist in Mg_2C_3, Me_4C_7 (Me = Y, Ho, Er, Tm, Lu), Sc_3C_4, and Ln_3C_4 (Ln = Ho − Lu) compounds [3,12–14]. The structures of Ln_3C_4 contain both $[C_3]$ and $[C_2]$ units, as well as isolated carbon atoms. Usually $[C_3]$ trimers are linear $[C = C = C]^{4-}$ groups with the C-C bond length of 1.34–1.35 Å (e.g., like in Mg_2C_3), which is close to that in gaseous allene (1.335 Å) [15]. However, the $[C_3]$ units in Sc_3C_4 and Ln_3C_4 structures are not linear. Hoffmann and Meyer [16] performed a fragment molecular orbital analysis to study the bonding characteristics of the $[C_3]$ units in Sc_3C_4 with the unusual bending (175.8°), the latter

attributed to the packing arrangement. Later, more binary carbides with Me_4C_7 compositions containing similar $[C_3]$ units, but with the bending angles of 167.8°—168.3°, were found [3,12].

High pressure alters the bonding patterns in carbides, leading to new compounds with unusual structural units and interesting properties, and as such, compression might enable exploring the catenation of carbon. Namely, for the binary systems Mg-C [17], Ca-C [18], Y-C [19,20], and La–C [2], an *ab initio* structure search predicts the formation of unusual metal carbides with exotic $[C_4]$, $[C_5]$ units and $[C_6]$ rings, graphitic carbon sheets, and a number of structural transitions. Carbon polymerization under high pressure can drastically change the physical properties of carbides and can lead, for example, to superconductivity [21,22].

At ambient pressure, the yttrium carbides family includes a large variety of binary phases with different stoichiometry and crystal chemistry [3]: Y_2C with isolated carbon atoms; YC_2 and Y_2C_3 with $[C_2]$ units; Y_3C_4 with $[C_3]$ units; Y_4C_5 with both single carbon atoms and $[C_2]$ units; Y_4C_7 with single carbon atoms and $[C_3]$ units. For Y_4C_5, two modifications are known: low-temperature α-Y_4C_5 and high-temperature β-Y_4C_5 [23]. Whereas the crystal structure of α-Y_4C_5 was solved and refined [space group *Pbam* (#55), $a = 6.5735(9)$, $b = 11.918(1)$, $c = 3.6692(5)$ Å] at ambient conditions [23], the structure of β-Y_4C_5 remains unknown. Under high pressure, only Y_2C_3 has been investigated [24–26]. Here, we report on the synthesis and characterization of a new high-pressure

modification of yttrium carbide, γ-Y_4C_5, with novel structure and very unusual crystal chemistry.

Results and discussion.—The γ-Y_4C_5 phase was first synthesized through a chemical reaction of yttrium with paraffin oil at ~44 GPa and ~2500 °C in the laser-heated diamond anvil cell (DAC1, Table S1 in the Supplemental Material [27]). The *in situ* synchrotron single-crystal x-ray diffraction enabled the crystal structure solution and refinement. The details of the sample preparation, data collection, structure determination, and refinement are described in the Supplemental Material [27]. To reproduce the synthesis of the γ-Y_4C_5 phase from the same precursors, two additional experiments were performed at ~46 GPa and ~2800 °C (DAC2), and at ~51 GPa and ~2500 °C (DAC3) [27]. In DAC2, only the known cubic Y_2C_3 phase [the Pu_2C_3-type structure, space group I-$43d$, $Z = 8$, $a = 7.745(4)$ Å] [27] was observed, which might be due to a different Y : C local ratio at the laser-heated spot. The γ-Y_4C_5 compound, which was also synthesized in DAC3, was gradually decompressed. At each pressure step of a few GPa, XRD data were collected to explore the behavior and the equation of state of γ-Y_4C_5. Reflections of the γ-Y_4C_5 phase were observed down to 16(2) GPa.

The γ-Y_4C_5 crystallizes in an orthorhombic structure (space group $Cmce$, $Z = 8$) with the unit cell parameters $a = 12.183(6)$, $b = 7.659(3)$, and $c = 8.858(2)$ Å at 44 GPa [Fig. 1(a)]. Full crystallographic information is provided in Table S2 [27]. Notable structural elements of the γ-Y_4C_5 are the diatomic $[C_2]$ (dimers or dumbbells), which lie in the bc plane, and triatomic $[C_3]$ units (trimers). If viewed along the b direction (see Fig. S1a [27]), the structure may be described as a series of layers of Y atoms stacked along the a direction. Every third layer includes the $[C_2]$ dimers alternating with Y atoms in the rows along the b direction. The $[C_2]$ dimers in the adjacent rows are mutually oriented in a "parquetlike" manner (see Fig. S1b [27]). The nonlinear $[C_3]$ trimers fill the space between the adjacent Y layers, which do not include dimers. The trimers form rows along the b direction. In each row, the summits of the trimers point to the same direction (see Fig. S1c [27]). The direction differs in each of two adjacent rows.

In the projection on the ac plane the trimers are turned with respect to each other and can be seen as crosses (see Fig. S1a [27]).

In the γ-Y_4C_5 structure, there are three crystallographically nonequivalent yttrium atoms with different coordination environment. The Y1 atoms possess the highest coordination number, CN = 10, with respect to the nearest carbon atoms, four of which belong to the two $[C_2]$ units in a side-on orientation, four to the two $[C_3]$ units, each giving two atoms, and two more carbon atoms come from the two end-on $[C_3]$ units (Fig. S1d [27]). The Y2 atoms have a CN of 6 with the contribution of one $[C_2]$ dimer in a side-on orientation, two more atoms- from two $[C_2]$ dimers in end-on orientation, and two atoms from the two end-on $[C_3]$ units (Fig. S1e [27]). The Y3 atoms are eight-fold coordinated (CN = 8) by two end-on $[C_2]$ dumbbells and by three differently coordinated $[C_3]$ units, as shown in Fig. S1f [27]. Such variation of yttrium coordination number in γ-Y_4C_5 is not unprecedented for yttrium carbides (see Table S3 [27] for the CN data for α-Y_4C_5, Y_4C_7, and Y_3C_4). However, C-C distances in $[C_2]$ dimers [1.40(2) Å] and $[C_3]$ trimers [1.43(1) Å] are unusual: they are significantly larger than expected for double-bonded carbon (~1.34 Å) and much shorter than for single-bonded (~1.54 Å) carbon atoms. They are not believed to be artifacts as the crystallographic data, including the C-C distance [1.32(1) Å, Table S4 [27]] obtained at ~46 GPa for the previously known cubic Y_2C_3 [21], are reasonable. Also, the significant bending of the triatomic carbon units (with the C3-C2-C3 angle of ~134°) in γ-Y_4C_5 calls for a more detailed analysis of the C-C bonds.

Upon decompression from 51 to 16 GPa, γ-Y_4C_5 expands quasi-isotropically (Fig. S2a [27]), and pressure-volume (P-V) data can be described by a second order Birch-Murnaghan equation of state (EOS) with the parameters $V_0 = 1016(8)$ Å^3 (the unit cell volume at ambient conditions) and $K_0 = 135(7)$ GPa (the bulk modulus) [Fig. 2(a)]. Unfortunately, the quality of the XRD data collected on decompression was insufficient to locate carbon atoms precisely, so that the changes in the C-C
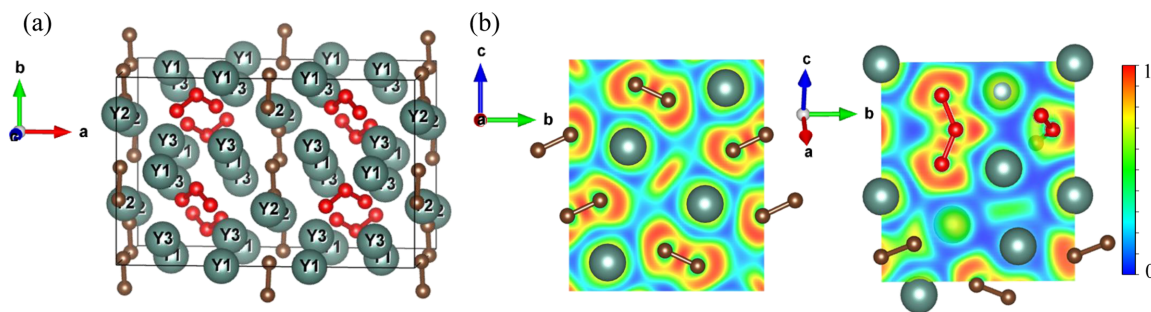
FIG. 1. Crystal structure of γ-Y_4C_5 at 44 GPa and corresponding 2D electron localization function (ELF) maps. (a) A unit cell of the structure with the Y atoms shown as gray and carbon atoms as brown and red balls, in dimers and trimers, respectively. (b) Cross sections of the calculated ELF shown in the planes containing the $[C_2]$ (left) and $[C_3]$ (right) units.

(a)

(b)
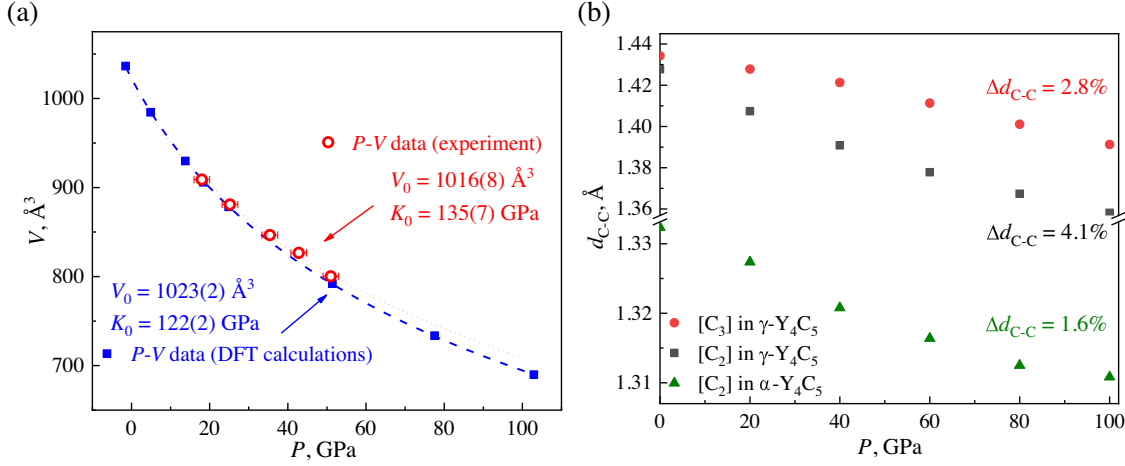
FIG. 2. Pressure dependence of the unit cell volume of γ-Y_4C_5 and the C-C distances ($d_{C\text{-}C}$) in the carbon units, for two Y_4C_5 polymorphs. (a) The P-V data for γ-Y_4C_5 obtained from XRD experiment and DFT calculations. The open red symbols represent experimental values of V in the decompression cycle for DAC3; the red dashed line shows the fit using the second order Birch-Murnaghan EOS. The blue solid symbols represent the P-V data resulted from DFT calculations; the blue dashed line is the corresponding second-order Birch-Murnaghan fit of the E-V data. (b) Pressure dependence of the calculated C-C distances in carbon units in α-Y_4C_5 and γ-Y_4C_5. The solid red circles, gray squares, and green triangles represent the C-C distances in the $[C_3]$ and $[C_2]$ units in γ-Y_4C_5, and the $[C_2]$ units in α-Y_4C_5, respectively. The relative change in the C-C bond length ($\Delta d_{C\text{-}C} = (d_{C\text{-}C(0\text{ GPa})} - d_{C\text{-}C(100\text{ GPa})})/d_{C\text{-}C(0\text{ GPa})}$) is 2.8% and 4.1% for the $[C_3]$ and $[C_2]$ in γ-Y_4C_5, and 1.6% for the $[C_2]$ in α-Y_4C_5.

distances in both dimers and trimers could not be traced. However, they were extracted from the relaxed structures obtained as a result of *ab initio* calculations using density functional theory (DFT).

The full relaxation of the structural model (at a volume corresponding to ~44 GPa) using DFT, as implemented in the plane wave VASP code [40], results in unit cell parameters and atomic coordinates which perfectly agree with the experiment (Table S1 [27]). The EOS parameters [$V_0 = 1024(1)$ Å^3 and $K_0 = 122(1)$ GPa] obtained from the computations based on energies from the optimization of the crystal structure of γ-Y_4C_5 over a wide volume range [Fig. 2(a)] are close to the experimental ones. The calculated bulk modulus of γ-Y_4C_5 is slightly larger than that of α-Y_4C_5 [$K_0 = 113(3)$ GPa], correlating well with the smaller volume per formula unit of γ-Y_4C_5 in comparison to α-Y_4C_5 (Fig. S3 [27]). According to the calculations, over the whole pressure range up to 100 GPa, the C-C distances in the $[C_3]$ units remain longer than in the $[C_2]$ dimers, but the C-C bonds in the dimers are almost 1.5 times more compressible than in the trimers [Fig. 2(b)]. It means that the dimers respond to compression by contraction, whereas the trimers partly adapt to the volume decrease through gradual bending. Indeed, in the pressure range from 0 to 100 GPa, the C3-C2-C3 bending angle changes from 139.6° to 133.5° (Fig. S2b [27]).

Harmonic phonon dispersion calculations using the Phonopy software [41] reveal that γ-Y_4C_5 is dynamically stable at its synthesis pressure of 44 GPa (Fig. S4 [27]), but is unstable at ambient conditions. The calculated electron density of states shows that high-pressure γ-Y_4C_5 is

metallic and the main contributions at the Fermi level come from the Y $4d$ and C $2p$ states (Fig. S5 [27]). In order to understand the stability range of γ-Y_4C_5, its enthalpy is compared with that of the known α-Y_4C_5, revealing that for $P > 12$ GPa γ-Y_4C_5 is thermodynamically favorable (Fig. S6 [27]). To explore the thermodynamic stability of γ-Y_4C_5 in comparison to other yttrium carbides, a convex hull was constructed for the binary Y-C system at different pressures considering known carbides [3,23,42]. The formation enthalpies of the compounds ($Y + xC \rightarrow YC_x$) are calculated relative to the DFT total energies of the end-member elements Y and C as $\Delta H_{Formation} = (H_{YCx} - H_Y - x \cdot H_C)/(1 + x)$. The γ-Y_4C_5 lies on the convex hull and therefore is thermodynamically stable for $P > 20$ GPa (Figs. 3 and S7 [27]), at least to the highest P explored (100 GPa).

To further explore the nature of the chemical bonding in γ-Y_4C_5 at 44 GPa, the computed charge density was analyzed in terms of the electron localization function (ELF) [43], which revealed strong covalent bonding between carbon atoms within the $[C_2]$ and $[C_3]$ units, and ionic bonds between Y and C (Fig. S8 [27]). Charge density maps in the planes containing the $[C_2]$ and $[C_3]$ units [Fig. 1(b)] show slightly larger ELF values between carbon atoms in dimers than in trimers. Therefore, one can assume a slightly higher bond order in the dimer, which correlates with experimentally obtained bond lengths.

Bader charge analysis [44] for Y1, Y2, and Y3 atoms yields values of 1.52, 1.25, and 1.51, respectively, in agreement with Bader charges for other yttrium carbides [45]. Notably, the lowest charge of 1.25 corresponds to the
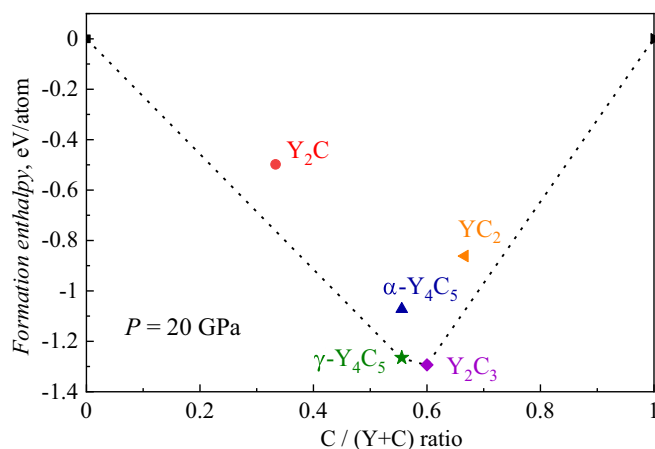
FIG. 3. The calculated convex hull in the Y-C binary-join for known yttrium carbides at 20 GPa. The phases γ-Y_4C_5 and Y_2C_3 lie on the convex hull (black dashed line) and are thus thermodynamically stable. Phases Y_2C, α-Y_4C_5, and YC_2 are off the convex hull and therefore unstable.

Y2 atom, with the smallest $CN = 6$, and, as a consequence, with the most limited Y to C charge transfer. The charges of carbon atoms C1, C2, C3, and C4 are -1.22, -0.78, -1.25, and -1.29, respectively, so that the edge carbon atoms in the trimer (C3) and in the dimer (C1 and C4) have similar charge states, while the charge for C2 at the center of the trimer is significantly smaller. According to our analysis of charge distribution in the ionic approximation based on a generalization of Pauling's concept of bond strength [46], made using CHARDI2015 [47], the carbon dimers and trimers have charges of -5.13 and -6.47, respectively. Full information on the charge distribution is summarized in Table S5 [27]. The obtained charge values for carbon units are unusually large, therefore to verify our results we performed charge calculations for Y_2C_3, YC_2, and α-Y_4C_5 yttrium carbides with known charge distribution (Table S6 [27]). Whereas the charges obtained for yttrium atoms in γ-Y_4C_5 and in Y_2C_3, YC_2, and α-Y_4C_5 compounds are almost the same and agree well with typical Bader charges for Y [45,48], the charges of carbon (and, as a consequence, of $[C_2]$ units) in γ-Y_4C_5 appear much larger (see Tables S5 and S6 [27]).

At ambient pressure, the low-temperature α-Y_4C_5 polymorph contains single carbon atoms and $[C_2]$ units, with a C-C bond length of 1.33 Å for $[C_2]$, which is equal to the double C-C bond in ethylene ($\sim$1.335 Å) [15]. This corresponds to a $[C_2]^{4-}$ dimer charge state and the formula of α-Y_4C_5 can be written as $Y_4^{3+}[C_2]_2^{4-}C^{4-}$ that is in a good agreement with charges calculated by the CHARDI method (Table S6 [27]). It is worth noticing here that the chemistry of rare earth metal carbides gives evidence that simple rules of electron counting do not describe these materials very well, so that no conclusion about their electronic properties, e.g., metallicity or non-metallicity, can be drawn directly from such assignments.

For the $[C_2]$ and $[C_3]$ units in γ-Y_4C_5, the C-C distances are 1.40(2) and 1.43(1) Å, respectively. They are longer than expected for double-bonded ($\sim$1.34 Å) and much shorter than for single-bonded ($\sim$1.50 Å) carbon atoms. The length of the C-C bond of the order of 1.5—like in benzene—is equal to 1.39 Å at ambient pressure, slightly shorter than both C-C bond lengths in γ-Y_4C_5. This leads us to the conclusion that the C-C bond orders in the $[C_2]$ and $[C_3]$ units are noninteger and should be in the range of 1.0–1.5.

Assuming that the $[C_2]^{Q1-}$ and $[C_3]^{Q2-}$ units have integer formal charges Q, the formula of γ-Y_4C_5 might be represented as $Y_4^{3+}[C_2]^{5-}[C_3]^{6-} \cdot 1e$, where the extra valence electron is delocalized in the conduction band, and does not participate in the Y-C or C-C bonding. The presence of delocalized valence electrons has been demonstrated for other binary metal carbides, e.g., for $Sc_3C_4 = Sc_{30}^{3+}[C_2]_2^{2-}[C_3]_8^{4-}C_{12}^{4-} \cdot 6e$ [14]. In this simple concept of charges' assignment, the new nonlinear $[C_3]^{6-}$ is an anion with 18 electrons, thus it is isoelectronic with the ozone O_3 molecule and the $[CBC]^{7-}$ anion in the $La_9Br_6(CBC)_3$ compound [49,50], both of which are also bent. The bending angles are naturally different for $[CBC]^{7-}$ ($\angle$C-B-C $= 148°$), $[C_3]^{6-}$ ($\angle$C-C-C $= 139.6°$), and O_3 ($\angle$O-O-O $= 116.8°$). Although the formal charge scheme for γ-Y_4C_5 is nice and even provides a simple interpretation for the C-C-C bending, it is inconsistent with the C-C bond lengths, and we suggest that the "spare" electrons contribute to the C-C bonding, and that the charges of the $[C_2]$ and $[C_3]$ units in γ-Y_4C_5 are noninteger. A similar phenomenon has recently been reported for $Na_3(N_2)_4$, where $[N_2]$ dimers have noninteger charges of -0.75 [51]. According to the charge analysis (Table S5 [27]), the Q_1/Q_2 ratio for $[C_2]^{Q1-}$ and $[C_3]^{Q2-}$ are very similar, regardless of the chosen analysis method. Assuming that the yttrium cation possesses its common charge Y^{3+}, and using the average ratio $Q_1/Q_2 = 0.775$, we obtain the following noninteger charges for the dimers and trimers $[C_2]^{5.24-}$ and $[C_3]^{6.76-}$ in γ-Y_4C_5. The noninteger charges of the carbon units can be explained by the delocalization of the electrons donated by Y atoms on the partially filled antibonding π^* molecular orbitals of the $[C_2]$ and $[C_3]$ units. The electrons transfer from yttrium to the carbon dumbbells is higher than to the trimers due to the shorter average distance between Y and C atoms in dimers (2.31 Å) in contrast to trimer (2.55 Å). This is in a good agreement with the averaged charges of -2.62 and -2.25 per carbon atom in dimers and trimers, respectively. The bond order is defined as a half of the difference between the number of bonding and of antibonding electrons, so for carbon anions $[C_2]^{5.24-}$ and $[C_3]^{6.76-}$, the bond orders are 1.38 and 1.31, respectively (Fig. S9, [27]). The noninteger formal charges of dimers are known for dinitrogen anions in recently synthesized compounds [51] and they obey the linear dependency between N-N bond length and charge state of $[N_2]^{x-}$. Here we explored
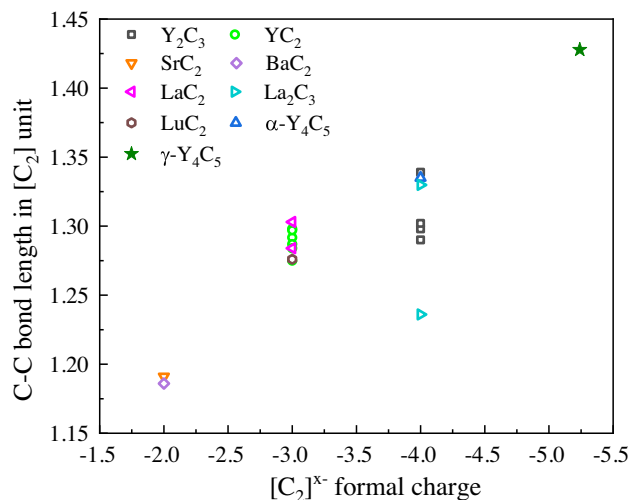
FIG. 4. Correlation between the C-C bond length and charges of the carbon dimers in binary metal carbides at 1 bar. For all presented carbides except γ-Y_4C_5, the C-C distances are those determined from experimental data [6,10,21,23,26,52–56], for γ-Y_4C_5 the value was obtained by DFT calculation from structure relaxation to 0 GPa.

the relationship between formal charges of dimers and the C-C interatomic distances for a number of metal carbides [6,10,23,52–56] and found an expected correlation between the two parameters: the C-C distance increases with an increase in the formal charge of the dimer (Fig. 4). Values predicted for γ-Y_4C_5 mainly match this trend, thus supporting our evaluation of the formal charge of $[C_2]$ as being high and non-integer.

Prior to this work, $[C_3]$ trimers have been considered as mainly linear $[C = C = C]^{4-}$ groups. Possible bending known so far does not exceed 15° (a bending angle of 167.8° was reported for Ho_4C_7) [12]—usually explained by denser packing arrangements in the structure. However, for γ-Y_4C_5, the C3-C2-C3 angle is 134.4(2)°, deviating from 180° by almost 50°, which cannot be explained by the packing arrangement alone. We suggest that the observed extreme bending is a result of pressure-induced charge transfer from Y d orbitals to antibonding states of $[C_3]$ units which leads to a decrease in the multiplicity of the C-C bonds and, as a result, the center C2 carbon atom cannot be considered as sp hybridized.

Conclusions.—The chemical reaction of yttrium and paraffin oil at pressures of ~50 GPa and temperatures of ~2500 °C led to the synthesis of a previously unknown polymorph of yttrium carbide, orthorhombic γ-Y_4C_5. The carbon atoms in the γ-Y_4C_5 crystal structure form $[C_2]$ dumbbells and nonlinear $[C_3]$ trimers with the unusual bending angle of 134.4(11)°. Density functional theory based calculations demonstrate the metallic nature of γ-Y_4C_5 and its dynamic stability at the synthesis pressures. They also indicate that above 12 GPa γ-Y_4C_5 is thermodynamically favorable relative to α-Y_4C_5. Noninteger

charges of carbon units, $[C_2]^{5.24-}$ and $[C_3]^{6.76-}$, determined by charge distribution analysis, can be explained by the delocalization of the electrons donated by Y on the partially filled antibonding π^* molecular orbitals of the $[C_2]$ and $[C_3]$ units. The partial filling of the antibonding π^* molecular orbitals of the $[C_3]$ unit results in an unusual C-C bond order of 1.31 and a considerable bending of the $[C_3]$ units. In this work we have demonstrated that covalently bonded carbon species can accommodate very large non-integer formal charges.

[*]Corresponding author.
Alena.Aslandukova@uni-bayreuth.de

[1] A. T. Santhanam, in *The Chemistry of Transition Metal Carbides and Nitrides*, edited by S. T. Oyama (Springer, Netherlands, 1996), https://dx.doi.org/10.1007/978-94-009-1565-7_2.

[2] C. Su, J. Zhang, G. Liu, X. Wang, H. Wang, and Y. Ma, Phys. Chem. Chem. Phys. **18**, 14286 (2016).

[3] V. Babizhetskyy, B. Kotur, V. Levytskyy, and H. Michor, *Handbook on the Physics and Chemistry of Rare Earths*, 1st ed (Elsevier B.V., New York, 2017), Vol. 52.

[4] L. E. Toth, *Transition Metal Carbides and Nitrides*, 1st ed. (Academic Press, New York–London, 1971).

[5] F. H. Spedding, K. Gschneidner, and A. H. Daane, J. Am. Chem. Soc. **80**, 4499 (1958).

[6] T. Sakai and G. Y. Adachi, T. Yoshida, and J. Shiokawa, J. Chem. Phys. **75**, 3027 (1981).

[7] R. E. Rundle, N. C. Baenziger, A. S. Wilson, and R. A. McDonald, J. Am. Chem. Soc. **70**, 99 (1948).

[8] M. Atoji, K. Gschneidner, A. H. Daane, R. E. Rundle, and F. H. Spedding, J. Am. Chem. Soc. **80**, 1804 (1958).

[9] M. Atoji and R. C. Medrud, J. Chem. Phys. **31**, 332 (1959).

[10] M. Atoji, J. Chem. Phys. **35**, 1950 (1961).

[11] R. West, I. A. Carney, and I. C. Mineo, J. Am. Chem. Soc. **87**, 3788 (1965).

[12] H. Mattausch, T. Gulden, R. K. Kremer, J. Horakh, and A. Simon, Z. Naturforsch. B **49**, 1439 (1994).

[13] H. Fjellvåg and P. Karen, Inorg. Chem. **31**, 3260 (1992).

[14] R. Pöttgen and W. Jeitschko, Inorg. Chem. **30**, 427 (1991).

[15] A. Almenningen, Acta Chem. Scand. **13**, 1699 (1959).

[16] R. Hoffmann and H. J. Meyer, J. Inorg. Gen. Chem. **607**, 57 (1992).

[17] T. A. Strobel, O. O. Kurakevych, D. Y. Kim, Y. Le Godec, W. Crichton, J. Guignard, N. Guignot, G. D. Cody, and A. R. Oganov, Inorg. Chem. **53,** 7020 (2014).

[18] Y. L. Li, S. N. Wang, A. R. Oganov, H. Gou, J. S. Smith, and T. A. Strobel, Nat. Commun. **6,** 6974 (2015).

[19] S. Roszak and K. Balasubramanian, J. Phys. Chem. **100,** 8254 (1996).

[20] X. Gao, Y. Jiang, R. Zhou, and J. Feng, J. Alloys Compd. **587,** 819 (2014).

[21] M. C. Krupka, A. L. Giorgi, N. H. Krikorian, and E. G. Szklarz, J. Less Common Met. **17,** 91 (1969).

[22] C. P. Poople, *Handbook of Superconductivity*, 1st ed. (Academic Press, San Diego, 2020).

[23] R. Czekalla, T. Hüfken, W. Jeitschko, R. D. Hoffmann, and R. Pöttgen, J. Solid State Chem. **132,** 294 (1997).

[24] G. Amano, S. Akutagawa, T. Muranaka, Y. Zenitani, and J. Akimitsu, J. Phys. Soc. Jpn. **73,** 530 (2004).

[25] S. Akutagawa and J. Akimitsu, Sci. Technol. Adv. Mater. **7,** 2 (2006).

[26] T. Nakane, T. Naka, H. Kito, T. Wada, A. Matsushita, H. Kumakura, and T. Mochiku, Physica (Amsterdam) **426–431C,** 492 (2005).

[27] See Supplemental Material at http://link.aps.org/supplemental/10.1103/PhysRevLett.127.135501 for experimental and theoretical calculations details, Tables S1–S6, Figs. S1–S8, and bibliography, which includes Refs. [28–39].

[28] I. Kantor, V. Prakapenka, A. Kantor, P. Dera, A. Kurnosov, S. Sinogeikin, N. Dubrovinskaia, and L. Dubrovinsky, Rev. Sci. Instrum. **83,** 125102 (2012).

[29] Rigaku Oxford Diffraction, CrysAlisPro Software system (2015).

[30] C. S. Zha, W. A. Bassett, and S. H. Shim, Rev. Sci. Instrum. **75,** 2409 (2004).

[31] S. Anzellini, A. Dewaele, F. Occelli, P. Loubeyre, and M. Mezouar, J. Appl. Phys. **115,** 043511 (2014).

[32] Y. Akahama and H. Kawamura, J. Appl. Phys. **100,** 043516 (2006).

[33] T. Fedotenko, L. Dubrovinsky, G. Aprilis, E. Koemets, A. Snigirev, I. Snigireva, A. Barannikov, P. Ershov, F. Cova, M. Hanfland, and N. Dubrovinskaia, Rev. Sci. Instrum. **90,** 104501 (2019).

[34] CrysAlisPro Data Collection, and Processing Software for Agilent X-Ray Diffractometers, Agilent Technol. Oxford (2014).

[35] V. Petrícek, M. Dušek, and L. Palatinus, Z. Krist. **229,** 345 (2014).

[36] K. Momma and F. Izumi, J. Appl. Crystallogr. **44,** 1272 (2011).

[37] J. Gonzalez-Platas, M. Alvaro, F. Nestola, and R. Angel, J. Appl. Crystallogr. **49,** 1377 (2016).

[38] J. P. Perdew, K. Burke, and M. Ernzerhof, Phys. Rev. Lett. **77,** 3865 (1996).

[39] G. Kresse and D. Joubert, Phys. Rev. B **59,** 1758 (1999).

[40] G. Kresse and J. Furthmüller, Phys. Rev. B **54,** 11169 (1996).

[41] A. Togo and I. Tanaka, Scr. Mater. **108,** 1 (2015).

[42] M. Atoji, R. C. Medrud, K. Gschneidner, A. H. Daane, R. E. Rundle, F. H. Spedding, K. Gschneidner, A. H. Daane, T. Sakai, G. Y. Adachi, T. Yoshida, J. Shiokawa, R. E. Rundle, N. C. Baenziger, A. S. Wilson, and R. A. McDonald, J. Chem. Phys. **80,** 99 (1958).

[43] A. Savin, A. D. Becke, J. Flad, R. Nesper, H. Preuss, and H. G. von Schnering, *Angew. Chem. Int. Ed. English* 30, 409 (1991).

[44] G. Henkelman, A. Arnaldsson, and H. Jónsson, Comput. Mater. Sci. **36,** 354 (2006).

[45] X. Feng, S. Lu, C. J. Pickard, H. Liu, S. A. T. Redfern, and Y. Ma, Commun. Chem. **1,** 85 (2018).

[46] L. Pauling, J. Am. Chem. Soc. **51,** 1010 (1929).

[47] M. Nespolo and B. Guillot, J. Appl. Crystallogr. **49,** 317 (2016).

[48] J. Chen, W. Cui, K. Gao, J. Hao, J. Shi, and Y. Li, Phys. Rev. Research **2,** 043435 (2020).

[49] H. Mattausch, A. Simon, C. Felser, and R. Dronskowski, Angew. Chem., Int. Ed. Engl. **35,** 1685 (1996).

[50] H. Mattausch and A. Simon, Angew. Chem., Int. Ed. Engl. **34,** 1633 (1995).

[51] M. Bykov, K. R. Tasca, I. G. Batyrev, D. Smith, K. Glazyrin, S. Chariton, M. Mahmood, and A. F. Goncharov, Inorg. Chem. **59,** 14819 (2020).

[52] V. Vohn, M. Knapp, U. Ruschewitz, V. Vohn, W. Kockelmann, and U. Ruschewitz, J. Solid State Chem. **151,** 111 (2000).

[53] M. Knapp and U. Ruschewitz, Chem. Eur. J. **7,** 874 (2001).

[54] V. Vohn, M. Knapp, and U. Ruschewitz, J. Solid State Chem. **151,** 111 (2000).

[55] Y. Yosida, J. Appl. Phys. **92,** 5494 (2002).

[56] M. Atoji and D. E. Williams, J. Chem. Phys. **35,** 1960 (1961).